Cationic Conjugated Polyelectrolytes with Molecular Spacers for Efficient Fluorescence Energy Transfer to Dye-Labeled DNA

ARTICLE *in* ADVANCED FUNCTIONAL MATERIALS · DECEMBER 2006

Impact Factor: 11.81 · DOI: 10.1002/adfm.200600093

6 AUTHORS, INCLUDING:

Doojin Vak
CSIRO (Australia)
42 PUBLICATIONS **1,535** CITATIONS

SEE PROFILE

FULL PAPER

ADVANCED FUNCTIONAL MATERIALS

DOI: 10.1002/adfm.200600093

Cationic Conjugated Polyelectrolytes with Molecular Spacers for Efficient Fluorescence Energy Transfer to Dye-Labeled DNA**

By *Han Young Woo*, *Doojin Vak*, *Dmitry Korystov*, *Alexander Mikhailovsky*, *Guillermo C. Bazan*,* and *Dong-Yu Kim**

Two water-soluble conjugated polyelectrolytes, poly(9,9′-bis(6-*N,N,N*-trimethylammoniumhexyl)fluorene-*alt*-1,4-(2,5-bis(6-*N,N,N*-trimethylammoniumhexyloxy))phenylene) tetrabromide (**P1i**) and poly((10,10′-bis(6-*N,N,N*-trimethylammoniumhexyl)-10H-spiro(anthracene-9,9′-fluorene))-*alt*-1,4-(2,5-bis(6-*N,N,N*-trimethylammoniumhexyloxy))phenylene) tetrabromide (**P2i**) are synthesized, characterized, and used in fluorescence resonance energy transfer (FRET) experiments with fluorescein-labeled single-stranded DNA (ssDNA-Fl). **P1i** and **P2i** have nearly identical π-conjugated backbones, as determined by cyclic voltammetry and UV-vis spectroscopy. The main structural difference is the presence of an anthracenyl substituent, orthogonal to the main chain in each of the **P2i** repeat units, which increases the average interchain separation in aggregated phases. It is possible to observe emission from ssDNA-Fl via FRET upon excitation of **P2i**. Fluorescein is not emissive within the ssDNA-Fl/**P1i** electrostatic complex, suggesting Fl emission quenching through photoinduced charge transfer (PCT). We propose that the presence of the anthracenyl "molecular bumper" in **P2i** increases the distance between optical partners, which decreases PCT more acutely relative to FRET.

1. Introduction

Conjugated polyelectrolytes are described by a backbone with a π-delocalized electronic structure and with pendant groups bearing ionic functionalities.[1] These materials combine the properties of polyelectrolytes, which are modulated by complex long-range electrostatic interactions, with the useful optical and electronic functions of organic semiconductors, which are determined to a large extent by interchain arrangements in the bulk. This set of properties has enabled applications in the design of biosensor schemes[2] and in the fabrication of optoelectronic devices.[3]

Cationic conjugated polyelectrolytes (CCPs) have been used to amplify the emission intensity from fluorophores bound to DNA, peptide nucleic acid (PNA), RNA, and peptides.[4–6] Their charged structures allow orchestration of electrostatic interactions such that fluorescence resonance energy transfer (FRET) from the CCP to the fluorophore occurs upon a specific recognition event. Thus, post FRET emission indicates the presence of a target species. By virtue of the larger absorption coefficient of CCPs, relative to their small-molecule counterparts, one obtains higher levels of sensitivity. It should be noted that the interaction of CCPs with negatively charged biomolecules results in the formation of aggregates, the structures of which remain poorly understood, and that need to be controlled so that the FRET process is optimized.[7] The molecular structure of the CCP must play an important role in determining the overall aggregate size, the distance between the optically active backbone and the acceptor dye, the local concentration of acceptor dyes, and the degree to which FRET or photoinduced charge transfer (PCT) takes place.

In this contribution, we report the design, synthesis, and photophysical properties of two new water-soluble CCPs, poly(9,9′-bis(6-*N,N,N*-trimethylammoniumhexyl)fluorene-*alt*-1,4-(2,5-bis(6-*N,N,N*-trimethylammoniumhexyloxy))phenylene) tetrabromide (**P1i**) and poly((10,10′-bis(6-*N,N,N*-trimethylammoniumhexyl)-10*H*-spiro(anthracene-9,9′-fluorene))-*alt*-1,4-(2,5-bis(6-*N,N,N*-trimethylammoniumhexyloxy))phenylene) tetrabromide (**P2i**), which are shown in Scheme 1. The main structural difference between the two CCPs is the presence of the anthracenyl substituent at the 9-position of the fluorene comonomer units in **P2i**, which is orthogonal to the backbone axis and serves to increase separation between chains in aggregated

[*] Prof. G. C. Bazan, Prof. H. Y. Woo, Dr. D. Vak, Dr. D. Korystov, Dr. A. Mikhailovsky
Departments of Chemistry and Materials
Institute for Polymers and Organic Solids
University of California
Santa Barbara, CA 93106 (USA)
E-mail: bazan@chem.ucsb.edu
Prof. D.-Y. Kim, Dr. D. Vak
Department of Materials Science and Engineering
Heeger Center for Advanced Materials
Gwangju Institute of Science and Technology
1 Oryong-dong, Buk-gu, Gwangju, 500-712 (Korea)
E-mail: kimdy@gist.ac.kr
Prof. H. Y. Woo
Department of Nanomaterials Engineering
College of Nanoscience and Nanotechnology
Pusan National University
Busan, 609-735 (Korea)

[**] The authors are grateful to the National Science Foundation, the Office of Naval Research and the National Laboratory program of KOSEF and BK21 program for financial support.

ADVANCED FUNCTIONAL MATERIALS

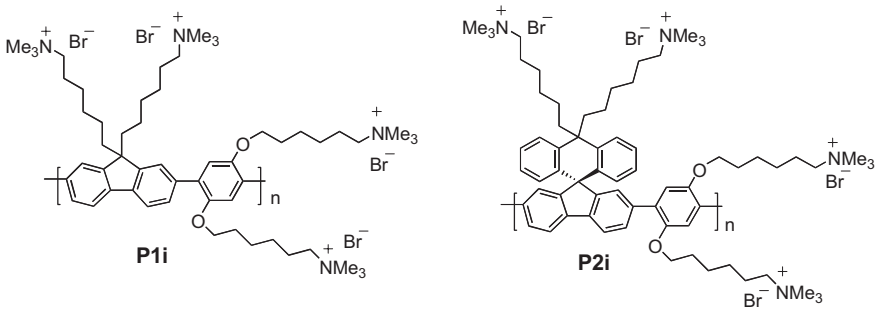

Scheme 1. Molecular structures of **P1i** and **P2i**.

phases. Such substitution does not perturb the π-conjugation on the backbone. As detailed below, the two polymers behave differently as excitation donors to fluorescein-labeled single stranded DNA (ssDNA-Fl). An examination of these differences provides insight into the intimate molecular interactions that favor FRET versus energy-wasting PCT. Optimized FRET processes lead to higher reported emission intensities and, ultimately, to more sensitive biodetection protocols.

2. Results and Discussion

The general synthetic entry into **P1i** and **P2i** is given in Scheme 2. Reaction of 6-chlorohexanol with *tert*-butylchlorodimethylsilane gives 6-chlorohexyloxy-*tert*-butyl-dimethylsilane (**1**) in 93 % yield. Spiro-substituted dibromofluorene, 10*H*-spiro(anthracene-9,9′-(2′,7′-dibromofluorene)) (**2**) was synthesized according to procedures reported previously[8] and was subsequently alkylated by reaction with **1**. Because of the lower reactivity of the hydrogens at the 10-position in dihydroanthracene relative to the 9-position in fluorene, it was not possible to introduce the modified alkyl chains by conventional methods.[7a,9] Instead, deprotonation of **2** with excess potassium hydride, followed by addition of **1**, gave 10,10′-bis(6-*tert*-butyldimethylsilyloxyhexyl)-10*H*-spiro(anthracene-9,9′-(2′,7′-dibromofluorene)) (**3**) in 75 % yield. Conversion of the terminal *tert*-butyldimethylsilyloxy group in **3** to bromide, to give 10,10′-bis(6-bromohexyl)-10*H*-spiro(anthracene-9,9′-(2′,7′-dibromofluorene)) (**4**), was performed using dibromotriphenyl phosphine (Br_2PPh_3) in dichloromethane at room temperature. The compound 10,10′-bis(6-bromohexyl)-10*H*-spiro(anthracene-9,9′-(2′,7′-bis(4,4,5,5-tetramethyl-1,3,2-dioxaborolan-2-yl)fluorene)) (**5**) is obtained by treating **4** with *n*-butyllithium and 2-isopropoxy-4,4,5,5-tetramethyl-1,3,2-dioxaborolane at –78 °C. 1,4-Bis(6-bromohexyloxy)-2,5-dibromobenzene (**6**), the comonomer common to both polymer structures, is readily obtained by deprotonation of 2,5-dibromobenzene-1,4-diol with KOH and subsequent alkylation with 1,6-dibromohexane. All compounds were characterized by ^1H and ^{13}C NMR spectroscopy and mass spectrometry.

Copolymerization of **5** or 9,9′-bis(6-bromohexyl)-2,7-bis(4,4,5,5-tetramethyl-1,3,2-dioxaborolan-2-yl)-fluorene (**5a**)[10] with **6** under Suzuki cross-coupling conditions using $Pd(PPh_3)_4$ in tetrahydrofuran (THF)/H_2O (2:1) under reflux over 24 h gives the neutral precursor polymers, poly(9,9′-

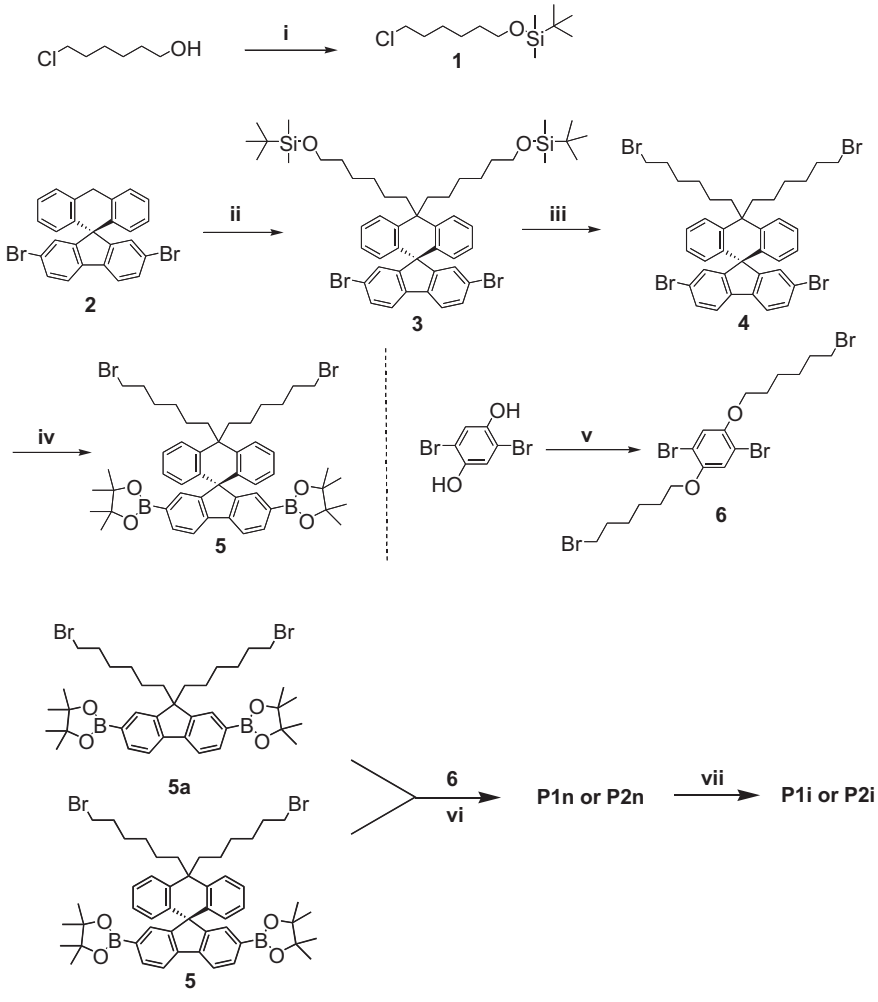

Scheme 2. Synthesis of **P1i** and **P2i**. Reagents and conditions: i) *tert*-butylchlorodimethylsilane, triethylamine, reflux, 1 h, $CHCl_3$; ii) **1**, KH, 18-crown-6, tetrahydrofuran (THF); iii) 0.33 M Br_2PPh_3 in CH_2Cl_2; iv) *n*-BuLi (*n*-butyllithium), 2-isopropoxy-4,4,5,5-tetramethyl-1,3,2-dioxaborolane, –78 °C, THF; v) 1,6-dibromohexane, tetrabutylammonium bromide, 80 °C, 45 % aqueous KOH; vi) $Pd(PPh_3)_4$, 2 M K_2CO_3, reflux in THF/H_2O, 24 h; vii) $N(CH_3)_3$, THF/H_2O, room temperature, 24 h.

bis(6-bromoexyl)fluorene-*alt*-1,4-(2,5-bis(6-bromohexyloxy))-phenylene) (**P1n**) and poly((10,10′-bis(6-bromohexyl)-10*H*-spiro(anthracene-9,9′-fluorene))-*alt*-1,4-(2,5-bis(6-bromohexyl-oxy))phenylene) (**P2n**) in ca. 60 % yields. Gel-permeation chromatography (GPC) analysis in chloroform, relative to polystyrene standards, provides number-average molecular weights of $M_n = 19\,000$ KDa (polydispersity index (PDI) = 1.42) for **P1n** and $M_n = 29\,000$ KDa (PDI = 1.69) for **P2n**. The water-soluble polymers **P1i** and **P2i** are obtained by treatment of **P1n** and **P2n** with condensed trimethylamine in a THF/water mixture for 24 h. After addition of trimethylamine, a precipitate gradually forms as the reaction proceeds, which is consistent with ionization of the pendant groups. To ensure reaction completion, it is recommended that the precipitate is redissolved by adding water (or methanol) and a further excess of trimethylamine. The degree of quaternization was estimated to be > 95 % from integration of the ^{1}H NMR spectra and a comparison of the peaks at ca. 3.1 ppm ($-N^+(CH_3)_3Br^-$) and at 4.1 ppm ($-OCH_2-$).

Figure 1 shows little difference in the absorption and photoluminescence (PL) maxima of **P1i** and **P2i** when measured in water. The absorption spectrum of **P2i** is slightly broader relative to that of **P1i**, which may be related to its lower solubility and thus its more pronounced tendency to aggregate.[11] Cyclic voltammetry (CV) measurements of **P1n** and **P2n** using a platinum working electrode in 0.1 M tetrabutylammonium hexafluorophosphate in acetonitrile at a scan rate of 10 mV s^{-1} revealed similar electrochemical oxidation potentials for both structures ($E_{ox} = 0.8$ V, relative to ferrocene). Therefore, the highest occupied molecular orbital (HOMO) and lowest unoccupied molecular orbital (LUMO) levels of the two polymers are nearly equienergetic. Similar PL quantum yields (Φ) were measured for **P1i** (0.43) and **P2i** (0.39), relative to fluorescein as a standard (in water at pH 11).

Single-stranded DNA, ssDNA-Fl, corresponding to the sequence 5′-fluorescein-ATCTT GACTA TGTGG GTGCT-3′, was used as a FRET acceptor in experiments involving excitation of **P1i** or **P2i**. Measurements were performed in water at pH 8. Fluorescein was chosen as the label as its absorption overlaps well with the emission of both polymers. Figure 2 shows the PL spectra of **P1i**/ssDNA-Fl and **P2i**/ssDNA-Fl solutions upon excitation of the polymers at 380 nm ([ssDNA-Fl] = 1.5×10^{-8} M, or [base] = 3×10^{-7} M; [**P1i**] = [**P2i**] = 3×10^{-7} M, based on polymer repeat units, RUs). It should be noted that the spectra are not normalized, thus they indicate that **P1i** and **P2i** are quenched to the same extent (since both have similar initial Φ values) and that the emission from Fl by FRET from **P2i** is considerably more efficient compared to the performance of **P1i**. It should also be noted that the more intense emission from Fl when using **P2i** instead of **P1i** is observed for all [RU]/[ssDNA-Fl] ratios tested under experimental conditions similar to those in Figure 2.

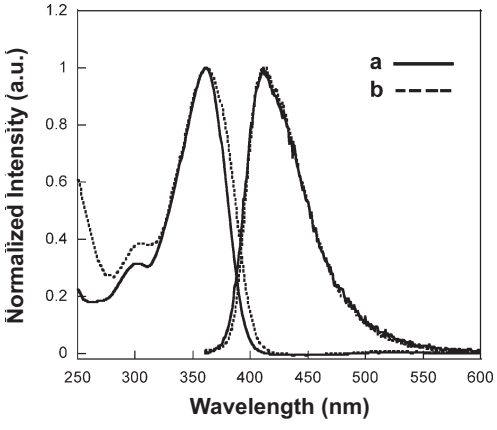

Figure 1. Normalized absorption and PL spectra of a) **P1i** and b) **P2i** in water.

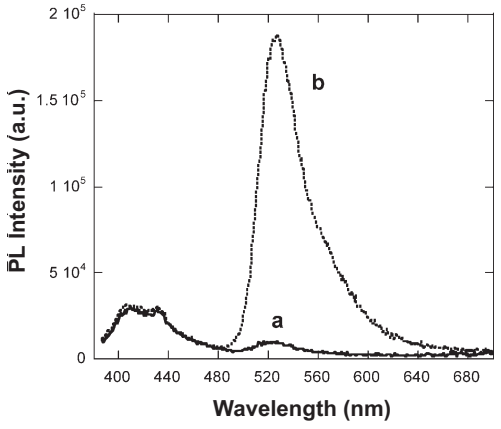

Figure 2. PL spectra of a) **P1i**/ssDNA-Fl and b) **P2i**/ssDNA-Fl in water at pH 8. ([ssDNA-Fl] = 1.5×10^{-8} M, [**P1i**] = [**P2i**] = 3×10^{-7} M). PL spectra were obtained by exciting at $\lambda_{ex} = 380$ nm. The spectra are not normalized.

Figure 3 displays the PL spectra obtained by *direct excitation* of Fl at 490 nm ([ssDNA-Fl] = 1.5×10^{-8} M) as a function of [**P1i**] or [**P2i**]. The Fl PL intensity decreases without a change in the emission maximum (λ_{PL}) as one increases [**P1i**]. When [**P1i**] = 3×10^{-7} M, Fl emission essentially disappears. Addition of **P2i** to ssDNA-Fl gives rise to a more gradual decrease of the Fl PL intensity. Fl emission can be clearly detected when [**P2i**] = 3×10^{-7} M. Significantly, addition of **P2i** results in a gradual red-shift of λ_{PL}, which indicates that the Fl is emissive when incorporated into the ssDNA-Fl/**P2i** complex.

The experimental conditions used to obtain the data in Figures 2 and 3 are similar to those used in DNA biosensor schemes, where accurate Φ values of free ssDNA-Fl and ssDNA-Fl/CCP complexes are difficult to obtain because of the dilute concentrations of these experiments ([ssDNA-Fl] $\simeq 10^{-8}$ M). Switching to more concentrated solutions ([ssDNA-Fl] = 10^{-6} M and [**P1i** or **P2i**] $\simeq 10^{-5}$ M), one observes results identical to those in Figure 2, i.e., the emissions of both polymers are quenched to the same extent upon ssDNA-Fl addition and the FRET efficiency by excitation of **P2i** is much larger than with **P1i**. Under these concentrations, the Φ values in the presence of ssDNA (of similar base-sequence composition to ssDNA-Fl) were determined to be 0.47 for **P1i** and 0.35 for **P2i** ([ssDNA] = 10^{-6} M; [**P1i**] = [**P2i**] = 1.5×10^{-6} M). Note that there is essentially no change in the Φ values when compared

ADVANCED FUNCTIONAL MATERIALS

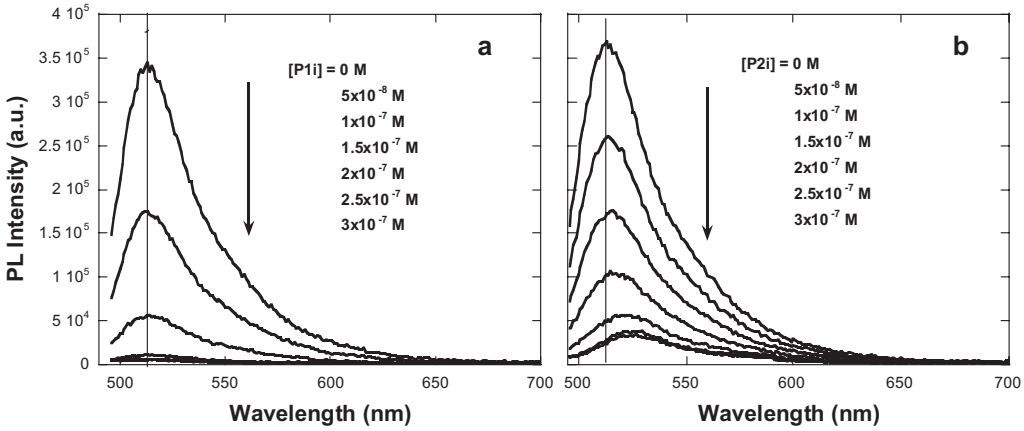

Figure 3. PL spectra of ssDNA-Fl ([ssDNA-Fl] = 1.5×10^{-8} M) with increasing [**P1i**] (a) or [**P2i**] (b) in water at pH 8. The spectra were measured by direct excitation of Fl at 490 nm; [**P1i**] = [**P2i**] = 0 to 3×10^{-7} M.

to the determination in the absence of ssDNA (Φ: 0.43 for **P1i** and 0.39 for **P2i**). Thus, we can infer that the lack of FRET to Fl in the case of **P1i** is not due to fluorescence self-quenching of the polymer upon complexation with ssDNA. It is also interesting to note that these results are different to those obtained with poly(9,9′-bis(6-*N*,*N*,*N*-trimethylammoniumhexyl)fluorene-*alt*-1,4-phenylene) dibromide,[12] for which complexation with DNA reduces Φ.

Figure 4 shows the absorption spectra of **P1i**/ssDNA-Fl and **P2i**/ssDNA-Fl in water at pH 8 ([ssDNA-Fl] = 10^{-6} M). The absorption maxima of **P1i** (λ_{abs} = 375 nm) and **P2i** (λ_{abs} = 369 nm) upon ssDNA-Fl complexation are red-shifted relative to free **P1i** (λ_{abs} = 362 nm) and **P2i** (λ_{abs} = 362 nm). Additionally, in both **P1i**/ssDNA-Fl and **P2i**/ssDNA-Fl the fluorescein absorption is red-shifted as a result of the change in the environment brought about by proximity to the cationic polyelectrolyte. This red-shift is slightly more pronounced with **P1i** (λ_{abs}(Fl): 494 nm → 507 nm) than with **P2i** (λ_{abs}(Fl): 494 nm → 502 nm), suggesting stronger complexation with **P1i**.

The fluorescein PL Φ in ssDNA-Fl in the presence and absence of **P1i** or **P2i** was measured upon direct excitation.[13]

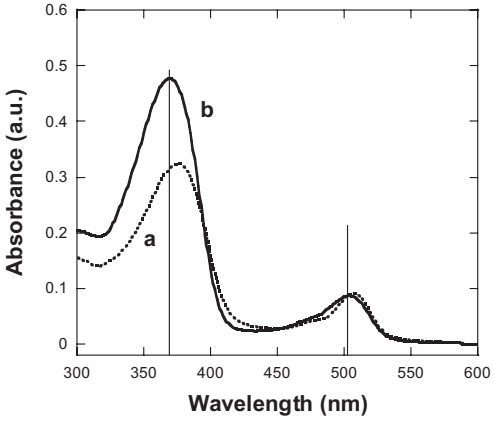

Figure 4. UV–vis spectra of a) **P1i**/ssDNA-Fl and b) **P2i**/ssDNA-Fl in water at pH 8. [**P1i**] = 1×10^{-5} M, [**P2i**] = 1.4×10^{-5} M, [ssDNA-Fl] = 10^{-6} M.

The Φ for ssDNA-Fl in water (at pH 8) is 0.8. After polymer complexation ([**P1i** or **P2i**] = 1.4×10^{-5} M and [ssDNA-Fl] = 10^{-6} M), the Φ values were determined to be 0.27 for **P2i**/ssDNA-Fl and approximately 0.01 for **P1i**/ssDNA-Fl. The PL Φ of Fl by **P2i** excitation (FRET-induced Φ) was calculated to be 0.16. Thus, the FRET efficiency in **P2i**/ssDNA-Fl can be approximated to be ca. 60 % by taking the ratio of the FRET-induced Φ over the direct fluorescein excitation Φ. For **P1i**/ssDNA-Fl this determination is not possible because of the low level of emission.

To summarize the observations described thus far, **P1i** and **P2i** have nearly indistinguishable spectroscopic features. Förster-type energy transfer from donor to acceptor through point dipole–dipole interactions is described by Equation 1[14]

$$k_{FRET} \propto \frac{\kappa^2}{r_{DA}^6} \int_0^\infty F_D(\lambda)\tilde{\alpha}_A(\lambda)\lambda^4 d\lambda \quad (1)$$

where k_{FRET} is the rate of energy transfer, κ relates to the relative transition moment orientation of donor and acceptor, r_{DA} is donor(D)–acceptor(A) distance; and the integral

$$\int_0^\infty F_D(\lambda)\tilde{\alpha}_A(\lambda)\lambda^4 d\lambda \quad (2)$$

expresses the spectral overlap between the donor emission, $F_D(\lambda)$, and the acceptor absorption, $\varepsilon_A(\lambda)$. Since the optical properties of the two polymers are similar, one would expect, based on Equation 1, similar levels of FRET efficiencies. However, as shown in Figure 2, the emission from ssDNA-Fl is much more intense with **P2i**. The weak emission of Fl for **P1i** and ssDNA-Fl is not due to polymer self-quenching prior to energy transfer, as shown by experiments where the polymer fluorescence is measured in the presence of ssDNA. There is also nearly complete Fl PL quenching upon direct Fl excitation in **P1i**/DNA-Fl, but relatively moderate quenching in **P2i**/DNA-Fl. Altogether, these considerations indicate that the fate of the polymer-based excitations is different and, by inference, that the differences in the molecular structures of the two polymers must play a critical role in determining the final optical outcome.

From the electrochemical measurements made by CV, and by taking into account the ionization potential 4.8 eV for ferrocene and the corresponding bandgap from absorption measurements, the HOMO and LUMO energy levels can be approximated.[15] For *both* **P1i** and **P2i**, the energies are estimated at –5.6 eV for the HOMO and –2.5 eV for the LUMO. Prior work has shown the HOMO and LUMO of fluorescein to be in the vicinity of –5.8 and –3.4 eV, respectively.[12,16] This order of energy levels leads to an energetically favored situation for excited-state quenching via PCT upon excitation of either the donor or the acceptor (Fig. 5).[12] However, despite the fact that the two polymers have a similar thermodynamic driving force for either FRET or PCT, it appears that PCT operates to a larger extent with **P1i**.

FRET and PCT rates, and thereby their probabilities, vary to different extents with the donor–acceptor distance. PCT is essentially a contact process described by an exponential distance dependence[17] and functions effectively at donor–acceptor distances considerably shorter than those probed by FRET processes (Eq. 1).[18] The nearly complete Fl emission quenching in **P1i**/ssDNA-Fl suggests that polymer excitation results in charge transfer to Fl.[19] With **P2i**/DNA-Fl, one observes much less Fl quenching, despite the similar optical properties of **P1i** and **P2i**. Our current thinking is that the introduction of the substituted 10*H*-spiroanthracenyl groups orthogonal to the backbone vector in **P2i** provides "molecular bumpers" that increase the average donor–acceptor distance. This increased separation reduces the probability of PCT relative to the parent **P1i** structure, but allows FRET to occur with good efficiency.

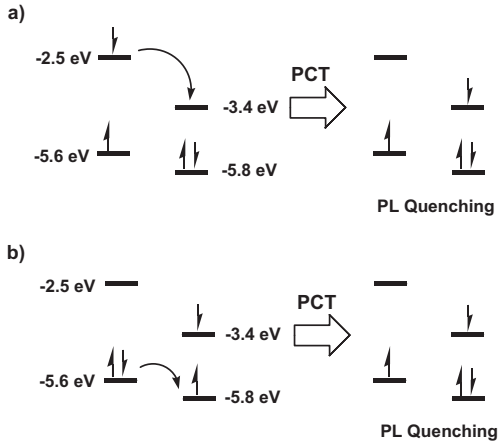

Figure 5. PL quenching via PCT by a) donor excitation and b) acceptor excitation.

3. Conclusions

We have reported the molecular design, synthesis, and examination of optical processes in the presence of fluorescein-labeled ssDNA for two water-soluble cationic conjugated polymers with similar electronic structures. The polymers have similar optical bandgaps and orbital energy levels, but differ in molecular structure, with **P2i** containing a molecular spacer (10*H*-spiroanthracenyl), which is lacking in **P1i**. For **P2i** it is possible to observe emission from ssDNA-Fl by FRET with a FRET efficiency of approximately 60 %. Fluorescein is not emissive within the ssDNA-Fl/**P1i** complex. We propose that the presence of the "molecular bumper" increases fluorescein emission by increasing the donor–acceptor distance, which decreases PCT quenching more acutely relative to FRET. We note that much effort has been devoted to improving the optical output in conjugated-polymer-based biosensors through improvements of polymer Φ and structural modifications that increase donor/acceptor spectral overlap. The results herein indicate that careful attention needs to be paid to molecular-design strategies that fine-tune distances at the molecular level to favor FRET over quenching by PCT reactions.

4. Experimental

Chemicals were purchased from Aldrich, and were used without further purification. Spiro-functionalized dibromofluorene (**2**) was synthesized by following previous procedures [8]. Oligonucleotides were purchased from Genscript Corp. and DNA concentrations were determined by measuring the absorbance at 260 nm in a 200 μL quartz cuvette. ssDNA-Fl is a 20 base-pair single-stranded DNA with a sequence of 5′-fluorescein-ATCTT GACTA TGTGG GTGCT-3′; ssDNA corresponds to the same sequence without the Fl labeling: 5′-ATCTT GACTA TGTGG GTGCT-3′. FRET experiments were performed by successive additions of polymers to a ssDNA-Fl solution in water at pH 8 and room temperature. ^{1}H and ^{13}C NMR spectra were collected on a Varian Unity 400 MHz (or 200 MHz) spectrometer. The UV–vis absorption spectra were recorded on a Shimadzu UV-2401 PC diode-array spectrometer. Photoluminescence spectra were obtained on a PTI Quantum Master fluorimeter equipped with a xenon lamp excitation source. Fluorescence quantum yields were measured relative to fluorescein and 9,10-diphenylanthracene [13]. Mass spectrometry was performed by the University of California Santa Barbara Mass Spectrometry Lab. Diagnostic characterization data for selected compounds follows:

1: ^{1}H NMR (200 MHz, $CDCl_3$): δ 3.50 (m, 4H), 1.70 (m, 2H), 1.40 (m, 6H), 0.84 (s, 9H), –0.01 (s, 6H) ppm. ^{13}C NMR (100 MHz, $CDCl_3$): δ 63.21, 45.25, 32.84, 26.90, 26.17, 25.35, 18.56, –5.08 ppm. MS (HREI): $(M–C_4H_9)^+ = 193.0824$ ($\Delta = 4.6$ ppm).

3: ^{1}H NMR (200 MHz, $CDCl_3$): δ 7.68 (d, 2H, $J = 6.6$ Hz), 7.47 (m, 4H), 7.23 (m, 2H), 7.05 (s, 2H), 6.90 (t, 2H, $J = 8.0$ Hz), 6.28 (d, 2H, $J = 8.0$ Hz), 3.52 (t, 4H, $J = 6.6$ Hz), 2.12 (m, 4H), 1.41 (m, 4H), 1.21 (br, 8H), 0.87 (m, 22H), 0.00 (s, 12H) ppm. ^{13}C NMR (100 MHz, $CDCl_3$): δ 159.81, 139.04, 138.10, 136.19, 130.59, 129.01, 128.54, 127.50, 126.25, 125.87, 122.30, 121.22, 63.24, 57.81, 46.72, 45.56, 32.74, 29.83, 25.99, 25.79, 25.58, 18.36, –5.27 ppm. MS (HREI): $(M–C_4H_9)^+ = 857.2406$ ($\Delta = 1.7$ ppm).

4: ^{1}H NMR (200 MHz, $CDCl_3$): δ 7.69 (d, 2H, $J = 8.0$ Hz), 7.48 (m, 4H), 7.25 (m, 2H), 7.04 (s, 2H), 6.92 (t, 2H, $J = 6.8$ Hz), 6.29 (d, 2H, $J = 8.0$ Hz), 3.33 (t, 4H, $J = 6.4$ Hz), 2.20 (m, 4H), 1.75 (m, 4H), 1.28 (m, 8H), 0.96 (m, 4H) ppm. ^{13}C NMR (100 MHz, $CDCl_3$): δ 159.72, 138.81, 138.10, 136.21, 130.63, 128.88, 128.60, 127.58, 126.35, 125.78, 122.29, 121.30, 57.77, 46.50, 45.58, 33.99, 32.58, 29.11, 28.02, 25.69 ppm. MS (HREI): $M^+ = 809.9697$ ($\Delta = 1.3$ ppm).

5: ^{1}H NMR (200 MHz, $CDCl_3$): δ 7.82 (m, 4H), 7.48 (d, 2H, $J = 7.6$ Hz), 7.34 (s, 2H), 7.17 (t, 2H, $J = 6.8$ Hz), 6.83 (t, 2H, $J = 6.8$ Hz), 6.27 (d, 2H, $J = 8.0$ Hz), 3.33 (t, 4H, $J = 7.0$ Hz), 2.21 (m, 4H), 1.75 (m, 4H), 1.5–1.0 (m, 36H) ppm.^{13}C NMR (100 MHz, $CDCl_3$): δ 157.97, 142.79, 138.84, 137.81, 133.93, 131.70, 129.55, 128.98, 126.70, 125.89, 125.52, 119.40, 83.45, 57.66, 46.84, 45.34, 33.54, 32.86, 29.06, 27.15, 25.07, 24.88 ppm. MS (HREI): $M^+ = 904.3260$ ($\Delta = 1.5$ ppm).

6: ^{1}H NMR (200 MHz, $CDCl_3$): δ 7.07 (s, 2H), 3.95 (t, 4H, $J = 6.2$ Hz), 3.42 (t, 4H, $J = 6.8$ Hz), 1.86 (m, 8H), 1.52 (br, 8H) ppm.

^{13}C NMR (100 MHz, $CDCl_3$): δ 149.95, 118.34, 111.07, 69.92, 33.78, 32.59, 28.86, 27.77, 25.14 ppm. MS (HREI): $M^+ = 589.8652$ ($\Delta = 2.4$ ppm).

P1n: ^{1}H NMR (200 MHz, $CDCl_3$): δ 7.85–7.50 (br m, 6H), 7.20 (s, 2H), 4.02 (m, 4H), 3.35 (m, 8H), 2.04 (br, 4H), 1.82–0.81 (br, 32H) ppm. $M_n = 19\,910$ KDa ($M_w/M_n = 1.42$).

P1i: ^{1}H NMR (200 MHz, DMSO-d_6): δ 7.97–7.60 (br m, 6H), 7.20 (s, 2H), 4.11 (br, 4H), 3.40 (m, 8H), 3.10 (br, 36H), 1.72–1.0 (br, 36H) ppm.

P2n: ^{1}H NMR (200 MHz, $CDCl_3$): δ 7.83 (d, 2H), 7.39 (br, 4H), 7.12 (br, 4H), 6.78 (m, 4H), 6.41 (d, 2H), 3.49 (br, 4H), 3.34 (t, 4H), 3.03 (t, 4H), 2.17 (br, 4H), 1.80–1.41 (br m, 10H), 1.30–0.80 (br, 22H) ppm. $M_n = 29\,600$ KDa ($M_w/M_n = 1.69$).

P2i: ^{1}H NMR (200 MHz, DMSO-d_6): δ 8.09 (br, 2H), 7.60–7.10 (br m, 8H), 6.91 (br, 4H), 6.22 (br, 2H), 3.56 (br, 12H), 3.05 (br, 36H), 2.18 (br, 4H), 1.80–0.7 (br m, 32H) ppm.

Received: January 15, 2006
Revised: April 2, 2006
Published online: December 13, 2006

[1] M. R. Pinto, K. S. Schanze, *Synthesis* **2002**, 1293.

[2] a) D. T. McQuade, A. E. Pullen, T. M. Swager, *Chem. Rev.* **2000**, *100*, 2537. b) B. Liu, G. C. Bazan, *Chem. Mater.* **2004**, *16*, 4467. c) K. P. R. Nilsson, O. Inganäs, *Nat. Mater.* **2003**, *2*, 419. d) M. R. Pinto, K. S. Schanze, *Proc. Natl. Acad. Sci. USA* **2004**, *101*, 7505. e) S. Kumaraswamy, T. Bergstedt, X. Shi, F. Rininsland, S. Kushon, W. S. Xia, K. Ley, K. Achyuthan, D. McBranch, D. Whitten, *Proc. Natl. Acad. Sci. USA* **2004**, *101*, 7511. f) H. A. Ho, M. Boissinot, M. G. Bergeron, G. Corbeil, K. Doré, D. Boudreau, M. Leclerc, *Angew. Chem. Int. Ed.* **2002**, *41*, 1548.

[3] a) F. Huang, L. Hou, H. Wu, X. Wang, H. Shen, W. Cao, W. Yang, Y. Cao, *J. Am. Chem. Soc.* **2004**, *126*, 9845. b) X. Gong, S. Wang, D. Moses, G. C. Bazan, A. J. Heeger, *Adv. Mater.* **2005**, *17*, 2053. c) W. L. Ma, P. K. Iyer, X. Gong, B. Liu, D. Moses, G. C. Bazan, A. J. Heeger, *Adv. Mater.* **2005**, *17*, 274. d) P. B. Balanda, M. B. Ramey, J. R. Reynolds, *Macromolecules* **1999**, *32*, 3970.

[4] a) B. S. Gaylord, A. J. Heeger, G. C. Bazan, *Proc. Natl. Acad. Sci. USA* **2002**, *99*, 10 954. b) B. S. Gaylord, A. J. Heeger, G. C. Bazan, *J. Am. Chem. Soc.* **2003**, *125*, 896.

[5] a) S. Wang, G. C. Bazan, *Adv. Mater.* **2003**, *15*, 1425. b) B. Liu, S. Baudrey, L. Jaeger, G. C. Bazan, *J. Am. Chem. Soc.* **2004**, *126*, 4076.

[6] S. J. Dwight, B. S. Gaylord, J. W. Hong, G. C. Bazan, *J. Am. Chem. Soc.* **2004**, *126*, 16 850.

[7] a) B. Liu, B. S. Gaylord, S. Wang, G. C. Bazan, *J. Am. Chem. Soc.* **2003**, *125*, 6705. b) M. A. Wolfert, P. R. Dash, O. Nazarova, D. Oupicky, L. W. Seymour, S. Smart, J. Strohalm, K. Ulbrich, *Bioconjugate Chem.* **1999**, *10*, 993.

[8] D. Vak, C. Chun, C. L. Lee, J.-J. Kim, D.-Y. Kim, *J. Mater. Chem.* **2004**, *14*, 1342.

[9] a) J. Lee, H.-J. Cho, B.-J. Jung, N. S. Cho, H.-K. Shim, *Macromolecules* **2004**, *37*, 8523. b) M. Fukuda, K. Sawada, K. Yoshino, *J. Polym. Sci. Part A* **1993**, *31*, 2465. c) T. Ahn, S.-Y. Song, H.-K. Shim, *Macromolecules* **2000**, *33*, 6764.

[10] S. Wang, B. Liu, B. S. Gaylord, G. C. Bazan, *Adv. Mater.* **2003**, *15*, 463.

[11] B. S. Gaylord, S. J. Wang, A. J. Heeger, G. C. Bazan, *J. Am. Chem. Soc.* **2001**, *123*, 6417.

[12] B. Liu, G. C. Bazan, *J. Am. Chem. Soc.* **2006**, *128*, 1188.

[13] a) A. Maciejewski, R. P. Steer, *J. Photochem.* **1986**, *35*, 59. b) S. R. Meech, D. Phillips, *J. Photochem.* **1983**, *23*, 193.

[14] J. R. Lakowicz, *Principles of Fluorescence Spectroscopy*, Kluwer Academic/Plenum Publishers, New York **1999**.

[15] a) J. Pommerehne, H. Vestweber, W. Guss, R. F. Mahrt, H. Bassler, M. Porsch, J. Daub, *Adv. Mater.* **1995**, *7*, 551. b) S. Janietz, D. D. C. Bradley, M. Grell, C. Giebeler, M. Inbasekaran, E. P. Woo, *Appl. Phys. Lett.* **1998**, *26*, 2453. c) S. H. Lee, B.-B. Jang, Z. H. Kafafi, *J. Am. Chem. Soc.* **2005**, *127*, 9071. d) L.-H. Chan, R.-H. Lee, C.-F. Hsieh, H.-C. Yeh, C.-T. Chen, *J. Am. Chem. Soc.* **2002**, *124*, 6469.

[16] M. Torimura, S. Kurata, K. Yamada, T. Yokomaku, Y. Kamagata, T. Kanagawa, R. Kurane, *Anal. Sci.* **2001**, *17*, 155.

[17] a) N. J. Turro, *Modern Molecular Photochemistry*, University Science Books, Sausalito, CA **1997**. b) J. Cornil, V. Lemaur, M. C. Steel, H. Dupin, A. Burquel, D. Beljonne, J.-L. Brédas, in *Organic Photovoltaics* (Eds: S. J. Sun, N. S. Sariciftci), Taylor and Francis, Boca Raton, FL **2005**, p. 161.

[18] a) S. Tyagi, F. R. Kramer, *Nat. Biotechnol.* **1996**, *14*, 303. b) M. K. Johansson, H. Fidder, D. Dick, R. M. Cook, *J. Am. Chem. Soc.* **2002**, *124*, 6950.

[19] PCT quenching has been observed with fluorescein "locked" within a protein environment by electron transfer from either a tryptophan or tyrosine residue, see: M. Götz, S. Hess, G. Beste, A. Skerra, M. E. Michel-Beyerle, *Biochemistry* **2002**, *41*, 4156.